SLOW DYNAMIC SLOPE METHOD IN INTERNAL COMBUSTION ENGINE BENCHMARKING

by

Nenad L. MILJIĆ**, *Slobodan J. POPOVIĆ, Predrag D. MRDJA, and Marko N. KITANOVIĆ

IC Engines Department, Faculty of Mechanical Engineering,
University of Belgrade, Belgrade, Serbia

Original scientific paper
https://doi.org/10.2298/TSCI170921226M

Enlarged engine control complexity made the full-factorial steady-state testing approach extremely time consuming and hardly applicable under actual industry demands. Slow dynamic slope (SDS) method is one of many approaches with a potential for considerable testing time savings, with its own benefits and drawbacks. This paper puts in focus SDS approach and evaluates its applicability, potentials and accuracy for fast estimation of engine steady-state maps. The presented research is based on an extensive experiment conducted on a small passenger car compresion ignition engine. Being the method that uses quasi-stationary sweeping of the engine, SDS test cycle durations in the range from 120-600 seconds are used in order to test the method and draw conclusions on its applicability. It is shown that well shaped SDS testing cycle can provide a rather good estimate of the steady-state operating points very quickly, with a negligible or very small loss of accuracy. The analysis is conducted both on fast responding variables and those that are heavily influenced by process inertia. This led to some suggestions on how to form a criterion for the SDS gathered data quality evaluation and SDS testing cycle correction.

Key words: *slow dynamic slope, dynamic internal combustion engine testing*

Introduction

Identification of internal combustion engine performance, its mapping and calibration are one of the key procedures in optimising the engine through its development. Within a scope of tremendous engineering efforts put in reducing the engine emission in last decades, the significance of engine maps optimisation has become even higher. The internal combustion engine (ICE) is the dominant propulsion technology of the present and the chance of its complete replacement in the upcoming decades is hardly imaginable. Relying on fossil fuels, ICE in road transport is responsible for cca. 17% of the world's CO_2 emission [1] and for cca. 12% in the EU [2]. Having other pollutants from fossil fuel combustion also in mind and fragile Earth's climate as an issue, research in the field of ICE is, more than ever, focused on its efficiency improvement and emission reduction toward fulfilment of targets already defined in regulatory frameworks worldwide.

It is well known that the steady-state engine testing approach is widely accepted almost as a golden standard with respect to its accuracy. On the other hand, enlarged engine

* Corresponding author, e-mail: nmiljic@mas.bg.ac.rs

control complexity, which introduced a lot of new control variables, made the steady-state approach extremely time consuming and thus hardly applicable under actual industry demands. Every steady-state measuring is comprised of three phases: a transient from the previous quasi-stationary state, stabilisation, and measurement phase [3]. Each phase requires some amount of time to be performed, which in overall puts a minimum of at least a few minutes to complete. It can be shown that with a so called full-factorial designed test with five control parameters and only fifteen operating points within a map, overall testing/calibration time through steady--state approach requires months of engine work on a test bed [4]. By implementing the (design of experiment) DoE concept of a carefully and model-based planned experiment, the number of needed operating points can be significantly reduced. While the DoE approach can reduce engine calibration time down to only a few weeks or less, an enormous number of simultaneously developed engine variants and time to market pressure forces higher demands on further engine calibration time cut-down [4].

On the other side, transient engine tests became far more interesting and needed in the optimisation phase since they are much closer to the realistic engine-in-powertrain behaviour. More realistic, highly dynamic driving cycles intended for engines legalisation are already in preparation for the final phase of release such as the EU WLTC (as a part of WLTP) [5] and its complementary real driving emissions [6]. This will further broaden and emphasize the significance of engine applicable dynamic models that can provide accurate enough and reliable means for successful and fast engine calibration through transient tests [7, 8]. With the state-of-the-art engine test bed automation systems, dynamic engine testing with transients are commonly used for identifying engine dynamical behaviour and building and validating dynamical models. They are further used for online and offline engine maps optimisation. Nonetheless, engine stationary maps are used intensively for control applications and the experience in dynamical testing has provided numerous methods and ideas on how to employ this faster testing approach in identifying engine's stationary operating points.

Ideas for using dynamic testing for stationary mapping of an engine are rather old [9]. Their main drawback is related to the fact that engine process non-linearities and inertia influence the response, which can significantly differ from the steady-state. The more rapid the excitation, the greater is the response deviation from the steady-state operating point. There are several approaches that are trying to overcome the aforementioned issue and provide more accuracy. One of them, so called *rapid measurement* focuses on the system identification method from the shortly recorded impulse excited transient. Online, quasi-continuously measured output data is used for adapting a dynamic statistical model that can estimate the final steady-state output value without the waiting time for the operating point stabilisation [10]. Another approach exploits an engine's response from a control parameter (s) sweep, usually conducted through a two-side linear ramp excitation. As it will be shown, the excitation ramp gradient is fundamentally related to the applicability of the recorded response to a satisfactory steady-state operating point's estimation. This ramp gradient should be limited to a *slow enough* angle, hence the name more commonly used in the literature – SDS testing.

It is well known that the SDS concept has its drawbacks, which are mostly evident in its inability to perform a good estimation of steady-state operating values of engine process variables with high thermodynamic inertia such as exhaust temperatures. Despite this fact, it appears to be very useful in fast sweeping of variable maps with low time constant values. The main goal of this paper is to present and discuss more in detail results of an extensive experiment dealing with the SDS method, since there are only a small number of publications that are explicitly dealing with it. In the experiment presented in this paper, the SDS method is used for

benchmarking of a well-known engine, *i. e.* an engine that has already been mapped through steady-state measurements and has a reference database on its mapping. Therefore, it will be possible to derive some conclusions on how the SDS approach to the engine mapping can be satisfactory both from the perspective of accuracy and testing time gain for various engine process variables.

The SDS method

The steady-state approach to engine operating point's measurement is conducted through several steps. A stepwise change of an input variable causes a transient that lasts some time, according to the process dynamic. Then, some time is required for the process to stabilize, which is followed by a steady operating point measurement. Overall time needed for completing all these steps is at least, 2-3 minutes for passenger car engines and 4-6 minutes for heavy-duty truck engines. Lagged behaviour of the engine is directly influenced by mechanical, fluidic and thermal dynamics of the engine and by the dynamics of measurement equipment [7]. If the system is excited by a ramp, then a quasi-stationary ramp measurement, *i. e. sweep measurement* can be performed.

By assuming that the system being considered is a first order system described:

$$T_1 \dot{y}(t) + y(t) = K u(t) \tag{1}$$

where T_1 and K are, respectively, the time constant and the gain of the system that is excited by a ramp input:

$$u(t) = \beta t \tag{2}$$

where parameter β represents the ramp gradient, the output $y(t)$, *i. e.* system response becomes:

$$y(t) = K\beta t - K\beta T_1 \cdot \left(1 - \mathrm{e}^{-t/T_1}\right) \tag{3}$$

It can be observed that the non-zero time constant, T_1, causes a system response time delay. The difference between delayed and non-delayed response ($T_1 = 0$) can be expressed:

$$\Delta y(t) = y(t, T_1 = 0) - y(t) = -K\beta T_1 \left(1 - \mathrm{e}^{-t/T_1}\right) \tag{4}$$

which, in time, tends to be a constant value:

$$\Delta y(\infty) = \lim_{t \to \infty} y(t) = -K\beta M T_1 \tag{5}$$

The offset is an unwanted but unavoidable component in the recorded engine response. It is obvious that it could be easily diminished by reducing the parameter β of the system input – a single parameter which can be influenced through experiment. Unfortunately, reducing the ramp gradient also means slower measurement and less time saving through the sweeping. On the other side, higher testing speed, *i. e.* steeper excitation ramp gradient, means greater deviation of the system response from the wanted one (fig. 1).

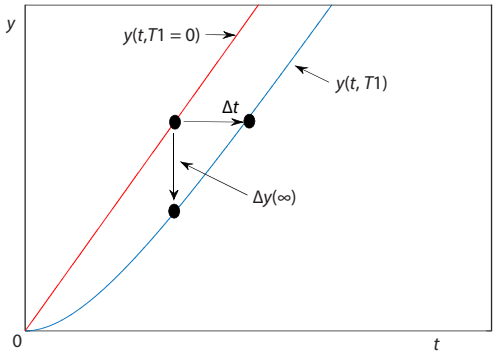

Figure 1. Measurement offset resulting from ramp excited first order system with time constant T_1

Ideally, in order to be used for the estimation of steady-state non-delayed output,

measured system output $y(t)$ should be corrected by compensation or elimination of the presented response offset. Keeping the excitation ramp slow enough diminishes the offset. If the offset is within the range of process disturbances and small in comparisons to process dynamics it can be neglected. Another approach compensates the offset by prolonging the system excitation with the symmetric negative gradient ramp. This produces an offset of opposite direction which, ideally, should cancel the one generated from the positive ramp excitation slope [7]. The latter method represents the SDS method.

How this applies, could be seen in fig. 2, where responses of two different first order system are shown. The systems are excited by the same ramp input, have the same gain, but different time constants. It is evident that the applied ramp gradient is far more appropriate for the excitation of the system with a smaller time constant ($T_1 = 2$ s). The offset of this system response is relatively small, giving small response hysteresis and a mean that is very well aligned with the non-delay response line.

Exciting a system with a slower response with the same ramp causes excessive response hysteresis on which the offset can be hardly compensated even with a symmetrical ramp excitation. Having in mind that the real processes in an engine can be treated as linear first order systems only upon significant simplifications, the response offset compensation issue becomes far more complicated in practice.

Processes in an engine are more or less influenced by heat transfer, mechanical and fluidic inertia, and thus behave as systems with variable gains and time constants through the engine operating range. This brings a question. Which of these processes, *i. e.* engine's output variables could be efficiently mapped through the SDS approach (where term *efficiently* means uncompromised accuracy compared to steady-state mapping data) with considerable testing time savings?

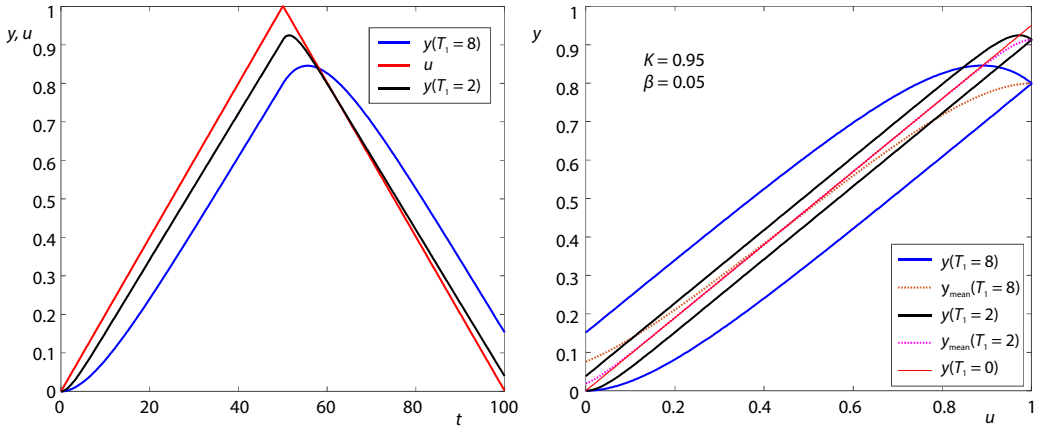

Figure 2. Examples of first order system responses with different time constants with the same ramp excitation (*for color image see journal web site*)

Engine test bed

The experiment was conducted on an engine test bench with details shown in figs. 3 and 4. Ramp like change of the engine torque is defined within the AVL Cameo test and measure environment through a series of test set points. Test bed system commands are further sent to the dyno and engine controller through the intermediate executive PC with an in-house developed LabVIEW application for synchronous data exchange between Cameo and dyno

controller. All measurements were synchronised and gathered through several data channels on a dedicated NI PXI system: measurements from various test bed-placed sensors (pressures and temperatures), measurements taken from the engine on-board diagnostic readings and data taken from the test bed automation system.

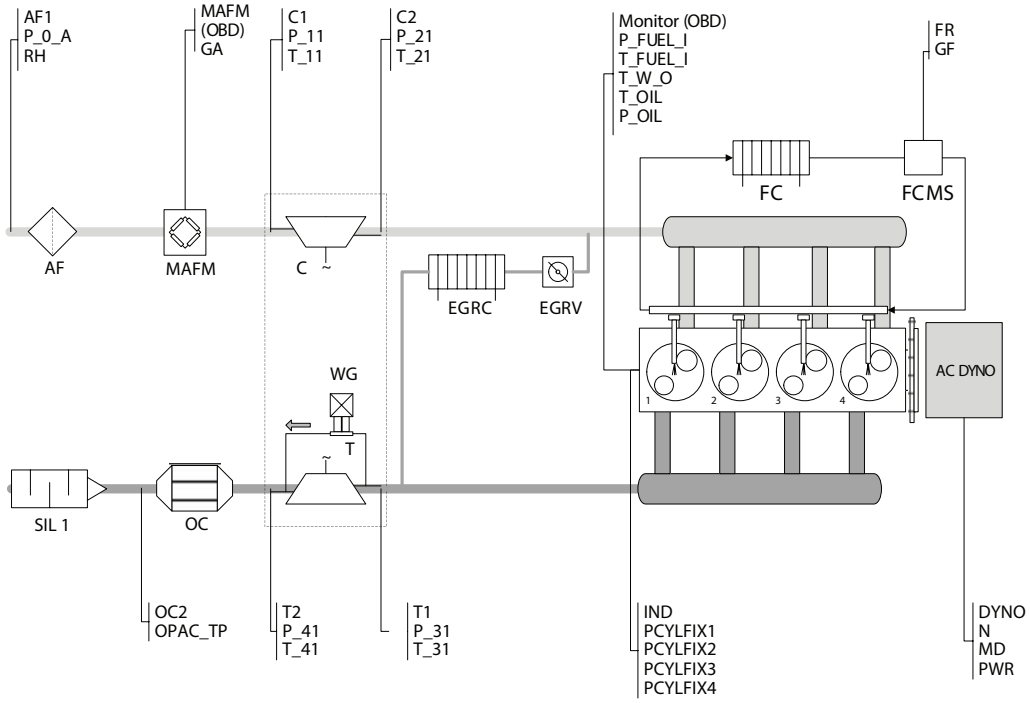

AF	Air filter	C	Compressor	OC	Oxi-Cat	IND	Indicating components	EGRC / V	Exhaust gas recirculation cooler / valve
MAFM	Mass air-flow meter	T / WG	Turbine / waste-gate	SIL	Silencer	FC	Fuel conditioner	FCMS	Fuel consumption measurement system

Name	Description	Sensor location	Engine	Data
P_0_A	Ambient absolute pressure	AF1	Manufacturer	PSA group
RH	Ambient air relative humidity	AF1	Model	DV4TD 8HT
GA	Mass air-flow	MAFM	Type	4 cylinder inline 4 stroke CI; 2 valves per cylinder; turbocharged, non -intercooled;
P_11; T_11	Compressor inlet air pressure; temperature	C1		
P_21; T_21	Compressor outlet air pressure; temperature	C2	Bore	73.7 mm
P_FUEL_I; T_FUEL_I	Fuel rail pressure; temperature	OBD	Stroke	84.0 mm
T_W_O	Engine coolant outlet temperature	OBD	Rated power	40 kW at 4000 min^{-1}
P_OIL; T_OIL	Engine oil pressure; temperature	Monitor	Rated torque	130 Nm
GF	Fuel mass-flow	FR	Fuel injection system	Common rail
N; MD	Engine speed; torque	DYNO	Turbocharger	KP35 (3K-BW)
PCYLFIX1-4	Cyl. 1-4 pressure indicating	IND	Bore	73.7 mm
P_31; T_31	Turbine inlet air pressure; temperature	T1	Stroke	84.0 mm
P_41; T_41	Turbine outlet pressure; temperature	T2		
OPAC _TP	Exhaust gas opacity	OC		

Figure 3. Engine test bed schematic

Additionally, an in-cylinder pressure indicating system was employed (AVL MicroI-FEM Piezo amplifiers & IndiMaster 670) with pressure sensors positioned in all four cylinders and a high-resolution encoder placed at the front of the crankshaft. Exhaust gas opacity was measured with the AVL 439 opacimeter (with a response time of 0.1 second).

The fuel consumption is measured with an in-house developed system FCMS-3000, which uses a gravimetric method through a hydrostatic pressure measurement of the fuel level in the measurement vessel. Measurement uncertainties of all measurement chains used were 0.5% or better.

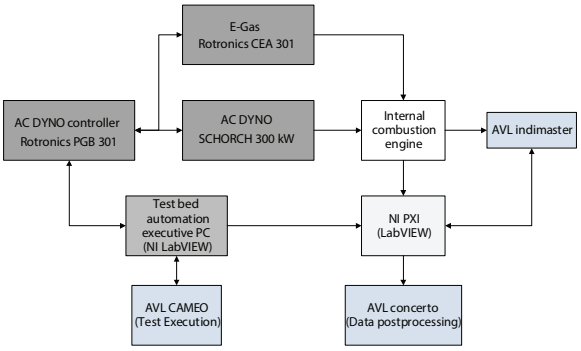

Test equipment	Model, Type, Description, Accuracy
Dynamometer	• Rotronics (ATB Schorch Asynchronous AC machine +Leroy Somer drivers); Pmax = 300 kW at 10000 rpm: Tmax = 700 Nn • HBM T40 2 kNm torque sensor; Accuracy class 0.05%
Indicating system	• AVL Indimaster 670 + MicroIFEM Piezo amplifiers • AVL 364C optical encoder, up to 0.1 deg. resolution • AVL GM12D piezoelectric uncooled pressure sensors (200 bar range. ±0.3% FSO linearity)
Opacimeter	• AVL 439, 0.01% sensitivity, 0.1 sec response time
Fuel consumption	• FCMS 3000, gravimetric mass-flow meter, Sensor combined linearity and hysteresis ±0.1% FSO; Sensitivity 0.02 g.
Data acquisition	• NI PXI system (PXI-8186 controller + PXI-6229 multifunctional card, 16-Bit, 250 kS/s) • (TC) NI SCXI 1102 + SCXI 1303, ±0.5°C CJC accuracy • (RTD) NI SCXI 1102 + SCXI 1581, ±0.1°C overall accuracy • Pressures: NI SCXI 1102 + IHTM piezoresistive sensors, ±0.1% FSO

Figure 4. Block schematic of the used engine test bed and data processing environment

Experimental set-up

Prior the SDS testing approach, the engine is stationary mapped through a series of load characteristics at 11 different engine speeds (fig. 5a) - at 950 and at 1200-3900 min^{-1} in 300 min^{-1} intervals, in overall amounting to 250 operating points.

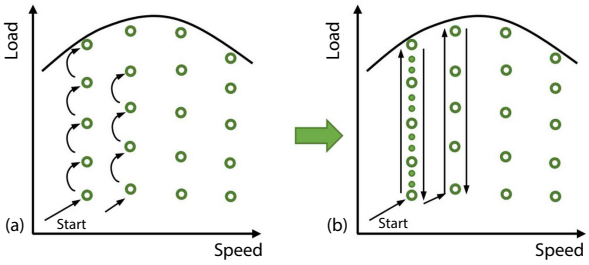

Figure 5. Mapping of the engine through steady-state and transient measurements; (a) stationary, (b) transient

In the transient part of the experiment, each of the engine load characteristics is swept with a symmetric linear torque ramp [11]. Constant speed testing is chosen deliberately for avoiding inertia induced torque and compensation related issues. In order to explore the differences and influences of the ramp gradients on the accuracy of steady-state estimates, each of the load characteristics is swept with several SDS ramp gradients with transient sweeping cycle durations ranging from 120-600 seconds. During each test cycle, eight engine variables were acquired as SDS responses: T_21, T_31, T_41, P_21, P_31, GF, IMEP, and exhaust gas opacity (parameter designation, fig. 3).

The testing cycle is comprised of two torque ramps and relatively short steady-state plateaus located before and after each of the ramp. The purpose of these plateaus stationarities is to, at least slightly, precondition the operating point before / after applying the ramp or change of the gradient. This approach is beneficial from the aspect of the SDS hysteresis evaluation since more data is gathered at the slope ends at a relatively small time-expense cost. Moreover, in order to start each of SDS cycles with a medium engine thermal load, mid value of maximum torque, at respective, engine speed, is chosen as a starting point. From the SDS methodology viewpoint, the starting point seems irrelevant, but the used approach showed some benefits in increased accuracy. Each SDS cycle is segmented in time domain as to establish sequences in

which engine operation is changed in a predefined way. The sequences are originally defined as follows:

– engine operation at half load (torque) at a given speed; the value of starting load is established as 50% of maximum torque measured in steady-state conditions at given speed,
– first positive ramp, in which the torque is increased with constant positive gradient from the starting value up to the maximum value for the given engine speed; the sequence duration, *i. e*. the torque ramp gradient is modified for different SDS cycle durations,
– steady-state operation at full load (maximum torque) at given engine speed,
– negative ramp, in which the torque is decreased with a constant negative gradient from the maximum torque at the given engine speed down to zero torque and further to the friction,
– line (negative torque, which varies with engine speed),
– second positive ramp, in which the torque is increased with constant positive gradient from the friction line up to the starting torque, as defined for the sequence No. 2, and
– repeated sequence No. 1.

Numerical designation for each SDS cycle is derived upon the sum of time duration for ramp sequences, *e. g.* for SDS cycle designated as SDS120, overall ramp time, both positive and negative, (Cycle *RT*) is 120 seconds, while overall cycle execution time (Cycle *ET*) is 150 seconds. Detailed time specification for each SDS cycle is presented in tab. 1.

Table 1. Applied SDS cycle characteristics: overall execution time and sequence duration

SDS cycle	Cycle *RT* [s]	Cycle *ET* [s]	Seq. #1 [s]	Seq. #2 [s]	Seq. #3 [s]	Seq. #4 [s]	Seq. #5 [s]	Seq. #6 [s]
SDS120	120	150	10	30	10	60	30	10
SDS220	220	250	10	55	10	110	55	10
SDS320	320	350	10	80	10	160	80	10
SDS420	420	450	10	105	10	210	105	10
SDS480	480	510	10	120	10	240	120	10
SDS540	540	570	10	135	10	270	135	10
SDS600	600	630	10	150	10	300	150	10

The torque data generated as set values for the dynamic tests realisation are presented in fig. 6. One can notice, both from tab. 1 and fig. 6, that the highest torque value remains steady for a limited period of approximately 10 seconds for all cycles, while at the very end of the negative ramp the steady sequence part is omitted. The reason for that comes from the control algorithm implemented in the used OEM engine electric control unit (ECU), which engages fuel cut-off during the negative ramp and thus disables precise control of the engine load.

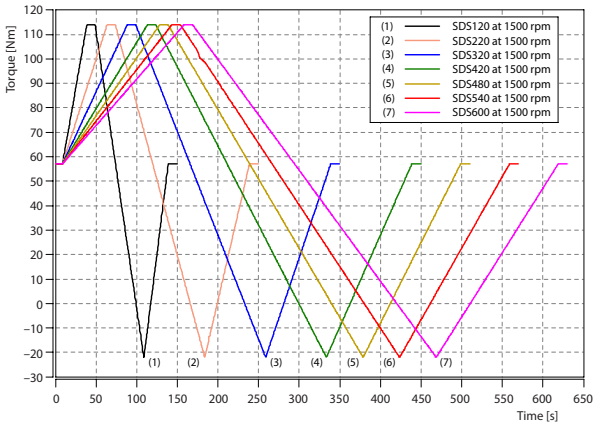

Figure 6. Torque ramps in SDS cycles; torque ramps range set up at 1500 min^{-1}

Data analysis

In order to evaluate the SDS data, some numeric evaluation and preprocessing is needed. Treated as a first order system response, measured data firstly has to be corrected with respect to the response offset. After low-pass filtration, response data is split in segments following the positive and negative torque ramp excitation, thus building the lower and upper part of the response hysteresis envelope. Since the symmetric excitation ramp is used, it is assumed that the response offsets are equal and opposite in sign, thus enabling the calculation of the system non-delayed estimate as a simple response hysteresis mean. The calculated mean then can be used as a substitute for a specific load characteristic series of steady-state.

A data pre-processing script, conducting the aforementioned calculations, is written in AVL Concerto data processing environment and placed into a macro block, which can be used from a convenient CalcGraph graphical data processing environment. This enables the evaluation of all SDS gathered data and generation of various steady-state map estimates in a matter of seconds.

Although convenient and relatively fast, the SDS approach for engine mapping imposes several questions that have to be answered first in order for the method to be used. Firstly – how steep should the ramp gradient be and, secondly, is the response of the particular engine output of interest fast enough to be acquired with the SDS?

Engine exhaust manifold temperature (T_31), and particularly an after-turbine one (T_41), can be considered as a relatively slow response variable. Figure 7(a) shows the SDS response of temperature T_31 at engine speed at 1500 min^{-1} upon the longest torque ramp cycle used in the experiment (RT = 600 seconds). It can be noticed, fig. 7(b), that the calculated hysteresis mean is in alignment with the reference steady-point values. By setting the accuracy limits on a lower, but acceptable level, this alignment could even be declared as a satisfactory steady-state estimation.

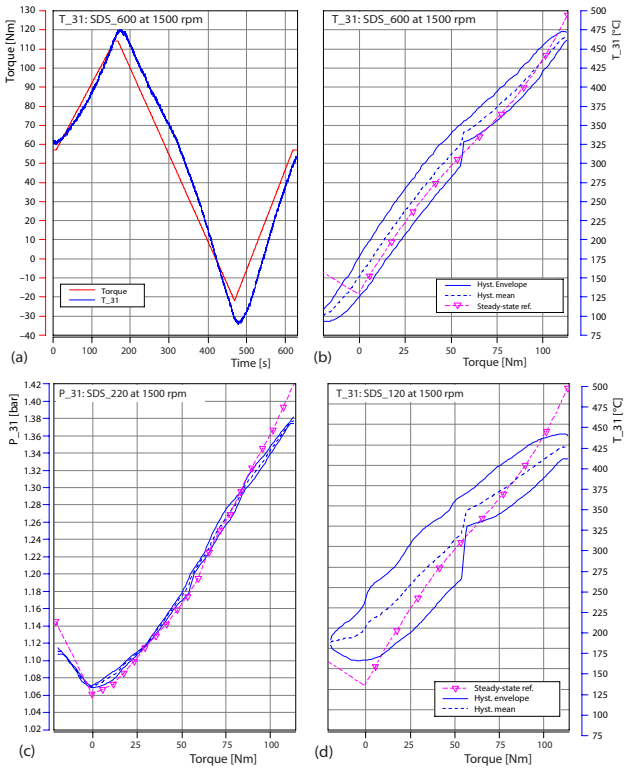

Figure 7. The T_31 and P_31 SDS responses at 1500 rpm (*for color image see journal web site*)

By applying the fastest torque ramp (RT = 120 seconds) the hysteresis becomes much larger with a mean that significantly deviates from the reference steady-state line. This is particularly evident in the higher and lower torque range where, obviously, the hysteresis mean can hardly be used as an accurate steady-state estimate, fig. 7(d). While the slow change of temperature is mostly influenced by the heat transfer inertia, the change of pressures in various segments of an engine are much faster processes. It can be seen, fig. 7(c) that, for an example, the turbine inlet pressure

(P_31) SDS response is rather fast and that hysteresis of this variable is small even with a high-speed torque ramp of RT = 120 seconds. A very good alignment of the hysteresis' mean and steady-state reference of this variable is apparent as well.

In general, it seems that fast responding variables can be efficiently mapped with the SDS method. Figure 8 presents the SDS response of the fuel mass-flow, fig. 8(a) and IMEP, fig. 8(b) at the steepest torque ramp gradient at 1500 rpm. It is evident that quasi-stationary acquisition of these variables can be achieved with negligible hysteresis and a very good alignment of its mean with the steady-state reference values, even with fast torque ramps. These results are in accordance with results from [12], where a 98 seconds throttle ramp time is used for successful dynamic estimation of the cylinder air charge on a gasoline engine. It is evident that short time spent at highest load, even with a plateau of 10 seconds is not enough to reach the stable highest load operating point. The same applies for the lowest load point and in both cases mainly due to sudden load change in these areas. This implies that envelopes of the engine operating field should not be derived from SDS data but, in addition, from separate lowest and highest load runs.

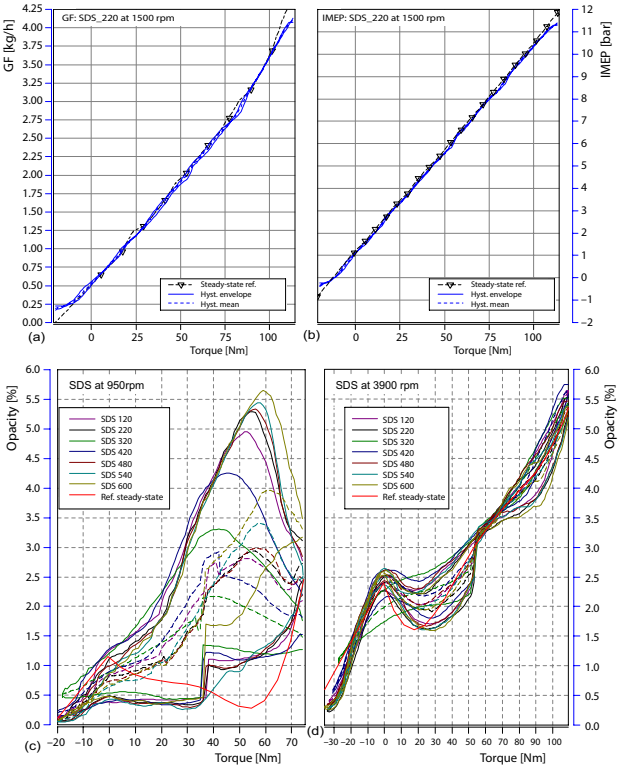

Figure 8. (a) Fuel mass flow, (b) BIMEP and opacity SDS responses (*for color image see journal web site*)

Figures 8(a) and 8(b) shows the SDS response of fuel mass-flow and IMEP measurements as valid response examples. On the other side, engine's response in exhaust gas opacity has a large time constant which is heavily influenced, as expected, by the air mass-flow, *i. e.* the engine speed. Figure 8(c) shows the opacity response at the lowest engine air-flow rates. It is very clear that hysteresis' means are almost uncorrelated to the steady-state measurements and that the SDS method can not be used for dynamic measurement of this variable – at least not with ramp times below 600 seconds. As air-flow rate increases, the SDS response expectedly improves, fig. 8(d). This implies that slow response variables do not provide consistent steady--state information quality through the complete engine's operating range. Of course, it can be assumed that with slower excitation ramps the quality of the response data can be improved significantly but at the expense of test time savings.

Following both the theoretical, figs. 1 and 2, and real system responses, figs. 7 and 8, one can assume that the span of the response hysteresis itself can be used as a validity indicator for determining the SDS response applicability in estimating steady-state operation data.

Nonetheless, there are several reasons why the hysteresis span value, *i. e.* the difference between the upper the lower hysteresis envelope, can not be used as a reliable validity indica-

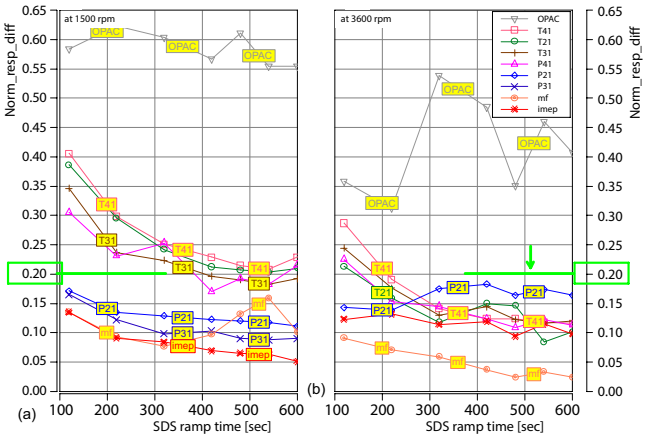

Figure 9. Normalized SDS excitation-response difference

tor. Firstly, hysteresis span varies through the SDS cycle and therefore only its average can be potentially used as a single numeric indicator which, in contrast, removes a lot of information on complete SDS cycle response. Secondly, if the system time constant is large compared to the excitation ramp time, the hysteresis span becomes almost irrelevant from the excitation ramp time and thus can hardly provide clear indication on the SDS gathered data validity even if the hysteresis span is small.

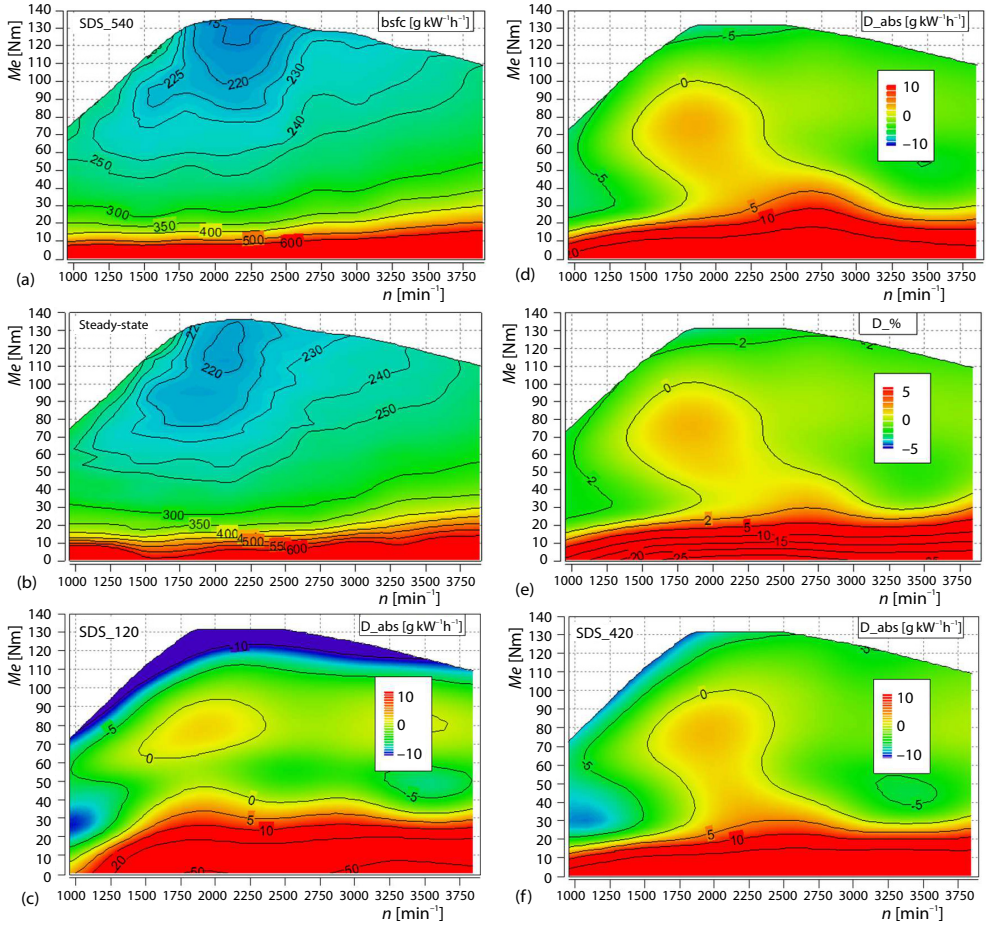

Figure 10. The BSFC map at *RT* = 540 seconds; (a) at steady-state, (b) and relative, (c) with absolute, (d) difference maps, (e) difference maps for *RT* = 120, and (f) 420 seconds (*for color image see journal web site*)

Upon analysis of all gathered data it is noticed that a more straightforward SDS response quality indicator can be derived from the normalised excitation and response data. Following the idea on estimation of the response offset of a pure first order system, the following difference can be calculated:

$$\Delta y_{\text{norm}}(t) = u_{\text{norm}}(t) - y_{\text{norm}}(t) \tag{6}$$

where $u_{\text{norm}}(t)$ and $y_{\text{norm}}(t)$ are excitation ramp and system response functions, respectively, normalised with the following function:

$$f_{\text{norm}}(t) = \frac{f(t) - \overline{f}(t)}{\max f(t) - \overline{f}(t)} \tag{7}$$

Difference function $\Delta y_{\text{norm}}(t)$ tracks the response offset, which reaches a maximum at a certain point. This maximum, if reached before the positive ramp peak (Seq. #2 from tab.1), is an analogue of the response offset limit explained in eq. (5) and fig. 1, and contains the information on the system time constant. It has been noticed that this parameter can be used as a good SDS response quality indicator.

By rule, a value of this parameter below 0.2 correlates well with *high quality* SDS runs, *i. e*. runs providing rather good alignment between calculated hysteresis mean and reference steady-state data. Figure 9 shows how this difference indicator varies with the ramp time as well as with the engine speed. This insight also explains why some variables' steady-state estimates can be predicted with higher accuracies at higher engine speeds only, when ramp time is fixed, or how this accuracy can be improved by introducing various ramp times over the engine speed range.

Another benefit of using this *rule of thumb* indicator is that it can be calculated in real-time, after finishing the second sequence of the SDS excitation cycle, thus providing prompt information and feedback on the applied ramp time, without the need for the SDS cycle to be completed.

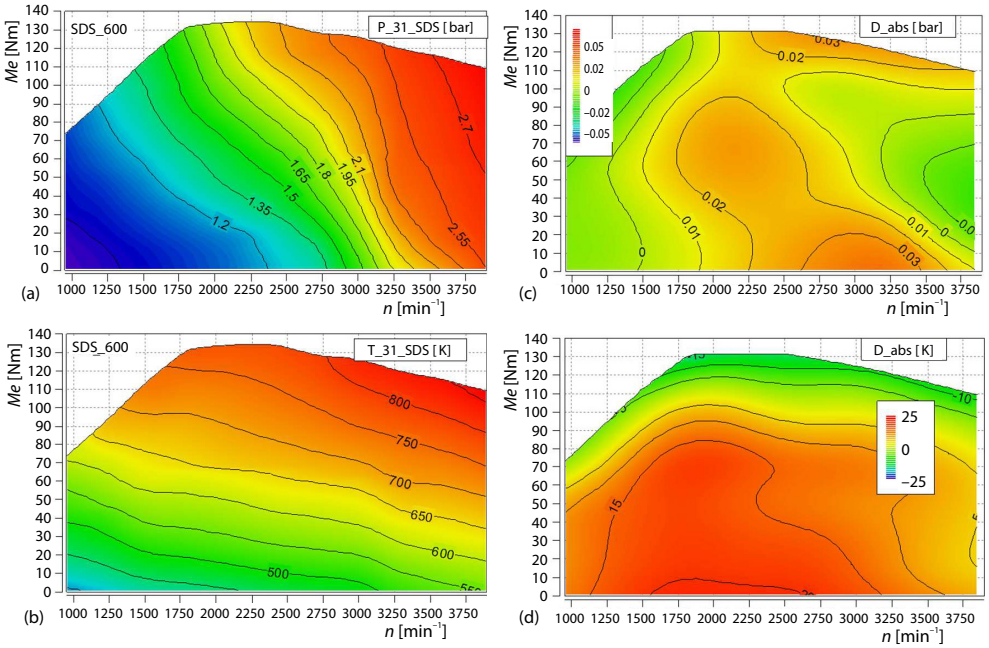

Figure 11. The P_31 (a) and T_31 (c) map at *RT* = 600 seconds with their steady-state difference maps (b) and (d) (*for color image see journal web site*)

For the purpose of load-speed engine mapping, engine operating range is swept with a number of constant speed SDS cycles. Gathered and post-processed data, is used for forming the estimates of steady-state maps. Figure 10 shows a fuel consumption map built from the SDS data, fig. 10(a), $RT = 540$ seconds, and from the reference steady-state data, fig. 10(b), as well as difference map in absolute, fig. 10(c), and relative, fig. 10(d), units. It can be seen that an absolute error in the steady-state estimate goes up to 10 g/kWh but only in a limited low torque region with higher BSFC values. Having in mind that an SDS sweeping procedure lasts about an hour, with $RT = 540$ seconds, and that a high-resolution steady-state measurement could last up to 10 times longer, it is clear that a huge amount of test time can be saved at the expense of a small or negligible accuracy loss. Figures 10(e) and 10(f) also shows the accuracy limits of faster SDS ramps ($RT = 120$ and 420 seconds) with a conclusion that faster dynamic testing does not necessary enlarge accuracy margins but spread inaccuracies wider through the operating range of the engine.

Figure 11 shows steady-state map estimates for variables P_31, fig. 11(a), and T_31, fig. 11(c), for $RT = 600$ seconds. Difference map for the fast response variable like P_31, fig. 11(b), shows neglectable accuracy loss while the slower one – temperature T_31, fig. 11(d), shows a noticeable but not an unacceptable accuracy loss.

Conclusions

Increasing complexity of ICE control puts high demands on engine map calibration and modelling. A large number of control variables exponentially increases the time needed for the engine control optimisation. This complexity further made steady-state full factorial engine calibration impossible to conduct in modern industry practice but has also motivated the rise of novel testing and calibration methods that can provide considerable testing time savings.

It is shown that quasi-stationary testing based on a symmetric ramp sweeping of engine can provide significant test time savings at negligible or small, but acceptable, accuracy loss. The SDS method can be successfully used for mapping and calibration of fast changing variables where pressures, fuel and air mass-flows are the most convenient candidates even with a sweep ramp times in the range of 100-150 seconds. Slower variables, highly influenced by inertia of the various engine processes, can also be mapped but with slower ramps chosen as a compromise between time test saving and acceptable accuracy loss. In a synergy with an efficient test automation and data processing system, the SDS method can save tremendous amount of testing time (up to 80%). The comparison is limited only to full factorial steady-state testing without any intention to avoid or neglect the significance of modern model-based DoE approach, which is used intensively as a method class of its own with a number of benefits but also a rather high complexity.

Developed calculation algorithm enables fast and convenient processing of SDS gathered data and generating of steady-state engine map estimates. Also, a validation criterion is identified as a rough quality indicator of the gathered SDS data. It can be monitored in real-time and used for early estimate of the applied SDS ramp effects on the engine's response.

Acknowledgment

The authors would like to thank AVL-List GmbH for their support of this research.

Acronymes

BSFC – brake specific fuel consumption
IMEP – indicated mean effective pressure
WLTC – worldwide harmonized light vehicles test cycles
WLTP – worldwide harmonized light vehicles test procedure

References

[1] ***, Publication: CO_2 Emissions from Fuel Combustion-2017, International Energy Agency (IEA), 2017
[2] ***, Regulation (EC) No. 443/2009 of the European Parliament and of the Council of 23 April 2009, Setting Emission Performance Standards for New Passenger Cars as Part of the Community's Integrated Approach to Reduce CO_2 Emissions from Light-Duty Vehicles, Europian Commision, 2009
[3] Deflorian, M., Experimental Design and Methods for the Identification of Continuous Time State Space Model as an Example of the Internal Combustion Engine (in German), Ph. D. thesis, Technical University of Munich, Munich, Germany, 2011
[4] Collette, Y., Planning of Experiments (in French), 2008, Available: http://ycollette.free.fr/Tools/Papers/Cours/01_Model_V3.pdf
[5] Tutuianu, M., *et al*., Development of the World-Wide Harmonized Light duty Test Cycle (WLTC) and a Possible Pathway for its Introduction in the European Legislation, *Transportation Research Part D: Transport and Environment*, *40* (2015), Supplement C, pp. S61-S75
[6] ***, Real-Driving Emissions in the EURO 6 Regulation on Emissions from Light Passenger and Commercial Vehicles (RDE3) – Regulation C(2017) 3720, June, 2017
[7] Isermann, R., *Engine Modeling and Control: Modeling and Electronic Management of Internal Combustion Engines*, Springer, New York, USA, 2014
[8] M. Paulweber, M., Lebert, K., *Powertrain Instrumentation and Test Systems: Development – Hybridization – Electrification,* Springer, New York, USA, 2016
[9] Godburn, J., D. *et al*., Computer-Controlled Non-Steady-State Engine Testing, *International Journal of Vehicle Design, 12*, (1991), 1, pp. 50-60, 1991
[10] Ropke, K., *et al*., Rapid Measurement, *MTZ Worldwide*, *68* (2007), 4, pp. 16-19
[11] Kock, K., The Challenge of New Measurement Methods for Fuel Consumption Measurement Devices on Engine Test Beds, *Proceedings*, Automotive Testing Expo North America 2008, Novi, Mich., USA, 2008
[12] Boehme, D., Methods for Efficient Basic Application of Air Path and Exhaust Gas Temperature Models in SI Engines (in German), Ph. D. thesis, VDI Verl., Dusseldorf, Germany, 2013

Paper submitted: September 21, 2017
Paper revised: October 22, 2017
Paper accepted: November 1, 2017